Open Journal of Modern Hydrology, 2026, 16(1), 66-83
https://www.scirp.org/journal/ojmh
ISSN Online: 2163-0496
ISSN Print: 2163-0461

# Development of Updated Intensity-Duration-Frequency (IDF) Curves Using Bias-Corrected IMERG Satellite Data for Urban Flood Management at the Bohicon Synoptic Station, Benin

**Peace S. Hounkpe[1,2], Joachim Tobada[1], Guy Oyéniran Adeoti[1,2], Brice Gbaguidi[3]**

[1]Doctoral School of Science, Technology, Engineering and Mathematics, Abomey, Benin
[2]National University of Science, Technology, Engineering and Mathematics, Abomey, Benin
[3]Doctoral School of Engineering Sciences, University of Abomey-Calavi, Abomey-Calavi, Benin
Email: adeotiguy@unstim.bj

**How to cite this paper:** Hounkpe, P.S., Tobada, J., Adeoti, G.O. and Gbaguidi, B. (2026) Development of Updated Intensity-Duration-Frequency (IDF) Curves Using Bias-Corrected IMERG Satellite Data for Urban Flood Management at the Bohicon Synoptic Station, Benin. *Open Journal of Modern Hydrology*, **16**, 66-83.
https://doi.org/10.4236/ojmh.2026.161005

**Received:** August 20, 2025
**Accepted:** December 23, 2025
**Published:** December 26, 2025



## Abstract

In the context of climate change and rapid urbanization, Beninese cities like Bohicon are increasingly exposed to frequent flooding. Estimating design flows for hydraulic drainage systems relies, among other tools, on intensity-duration-frequency (IDF) curves. This study aims to construct IDF curves for the Bohicon synoptic station using bias-corrected IMERG satellite rainfall data calibrated with local ground measurements. Maximum rainfall intensities extracted from a 23-year dataset (2000-2023) were fitted to several extreme value probability distributions, including the Gumbel and Weibull distributions, with coefficients of determination ($R^2$) reaching 0.98 for the best fits. Three empirical models—Montana, Keifer-Chu, and Talbot—were tested for constructing the IDF curves. The results show that the Talbot model offers the best statistical performance for all return periods (2 - 100 years), with an RMSE of less than 5 mm/h for T = 2 years and less than 25 mm/h for T = 100 years, reflecting low error and satisfactory reliability of the adjustments, especially for short to medium return periods. For example, for a one-hour rainfall duration and a 10-year return period, the estimated intensity reaches 84 mm/h, compared to 62 mm/h with historical curves. These new IDF curves, calibrated locally and incorporating recent precipitation variability, provide more accurate estimates of extreme rainfall intensities over different durations. They are therefore particularly well-suited to the hydraulic design of urban drainage systems in Bohicon. This research offers a modern and reliable alternative to the historical IDF curves developed by the Inter-African Committee for Hydraulic Studies [1], which were based on limited and outdated rainfall data. The proposed curves provide an updated and robust basis for hydrodynamic flood simulation and resilient urban planning in the face of hydroclimatic extremes.


## Keywords

IDF Curves, IMERG, Urban Drainage, Bohicon, Hydrological Design, Flood Risk


## 1. Introduction

Under the combined effects of climate change and poorly managed urbanization, West Africa has become one of the regions most affected by the growing recurrence of urban flooding. Each year, intense rainfall events trigger sudden flash floods that are particularly destructive in urban centers such as Bohicon, where existing stormwater drainage systems struggle to meet current hydrological demands.

In response to these challenges, the World Meteorological Organization [2] recommends integrated flood risk management strategies based on reliable and up-to-date hydroclimatic data. One of the most essential tools for hydraulic infrastructure design is the Intensity-Duration-Frequency (IDF) curve, which provides estimates of extreme rainfall intensities for various durations and return periods.

However, in many West African engineering projects, IDF curves still in use today were developed several decades ago, primarily by the Inter-African Committee for Hydraulic Studies [1]. These curves were established using limited historical data, and they do not account for recent climatic variability or short-duration rainfall events (*i.e.*, durations less than 1 hour), which are now recognized as critical for triggering urban surface runoff.

As highlighted by [3], several extreme rainfall events recorded since the 1990s—particularly in 2010 and 2013—have significantly exceeded the intensities projected by the outdated curves, thus calling into question their validity for infrastructure design in a changing climate.

Despite its strategic role in Benin's urban network, the city of Bohicon lacks long-term high-resolution local rainfall time series. In this context, data from the IMERG (Integrated Multi-satellite Retrievals for GPM) satellite product present a promising alternative. With high spatial and temporal resolution (up to 30-minute intervals) and global continuous coverage, IMERG data can compensate for the lack of ground observations—provided they are locally bias-corrected using in situ measurements to ensure their reliability and representativeness.

This study aims to construct updated and locally calibrated IDF curves for the Bohicon synoptic station, using IMERG satellite rainfall data corrected with local ground observations. The broader objective is to update hydrological design parameters for urban areas in the face of climate-driven shifts in precipitation regimes. The specific objectives are:

1) To fit the series of maximum rainfall intensities to extreme value probability distributions.

2) To test and compare the performance of three empirical models—Montana, Keifer-Chu, and Talbot—for constructing IDF curves.

3) To generate reliable and up-to-date IDF parameters to support the optimized design of urban drainage infrastructure in Bohicon.

Through this approach, the study provides a technically robust alternative to outdated historical references and lays the groundwork for hydraulic modeling and flood risk reduction in Benin's urban environments.

## 2. Methodology

### 2.1. Study Area

The Hlan watershed is located in the south-central region of Benin, between approximately 7˚07'N and 7˚29'N latitude and 1˚95'E and 2˚15'E longitude. It spans an estimated surface area of 560 $km^2$ and straddles two major urban agglomerations: Bohicon and Abomey, respectively the second and fourth most populated cities in the Zou Department. The watershed plays a vital hydrological role in draining stormwater runoff from these urban centers, particularly in a context of rapidly increasing soil imperviousness due to urban expansion (**Figure 1**).

The climate of the region is classified as Sudano-Guinean, characterized by a bimodal rainy season with a primary peak in rainfall occurring between April and July, and a secondary peak between September and October. Annual rainfall typically ranges from 1000 to 1200 mm, with daily intensities often exceeding 50 mm/day during extreme precipitation events [4]. This climatic regime, combined with unregulated urban growth, makes the area especially vulnerable to urban flooding.

Rainfall data recorded at the Bohicon synoptic station between 1980 and 2023 reveal high interannual variability in the number of rainy days. A downward trend is observed after the year 2000, which suggests a shift in rainfall patterns—reduced frequency of rainfall events coupled with increased intensity—consistent with the impacts of climate change (see **Figure 2**).

Moreover, monthly average rainfall distribution shows peak precipitation levels in June and September, with values gradually tapering off in the dry season (November to February). This rainfall pattern (**Figure 3**) further confirms the bimodal structure of the regional rainfall regime, which has critical implications for hydrological modeling and infrastructure design in the study area.

### 2.2. Data and Methods

This study utilizes satellite-based precipitation data from the IMERG Final Run V07B product, developed under NASA's Global Precipitation Measurement (GPM) mission. The data offer a temporal resolution of 30 minutes and a spatial resolution of 0.1˚ × 0.1˚ (approximately 10 km × 10 km), covering the period from 2000 to 2023.

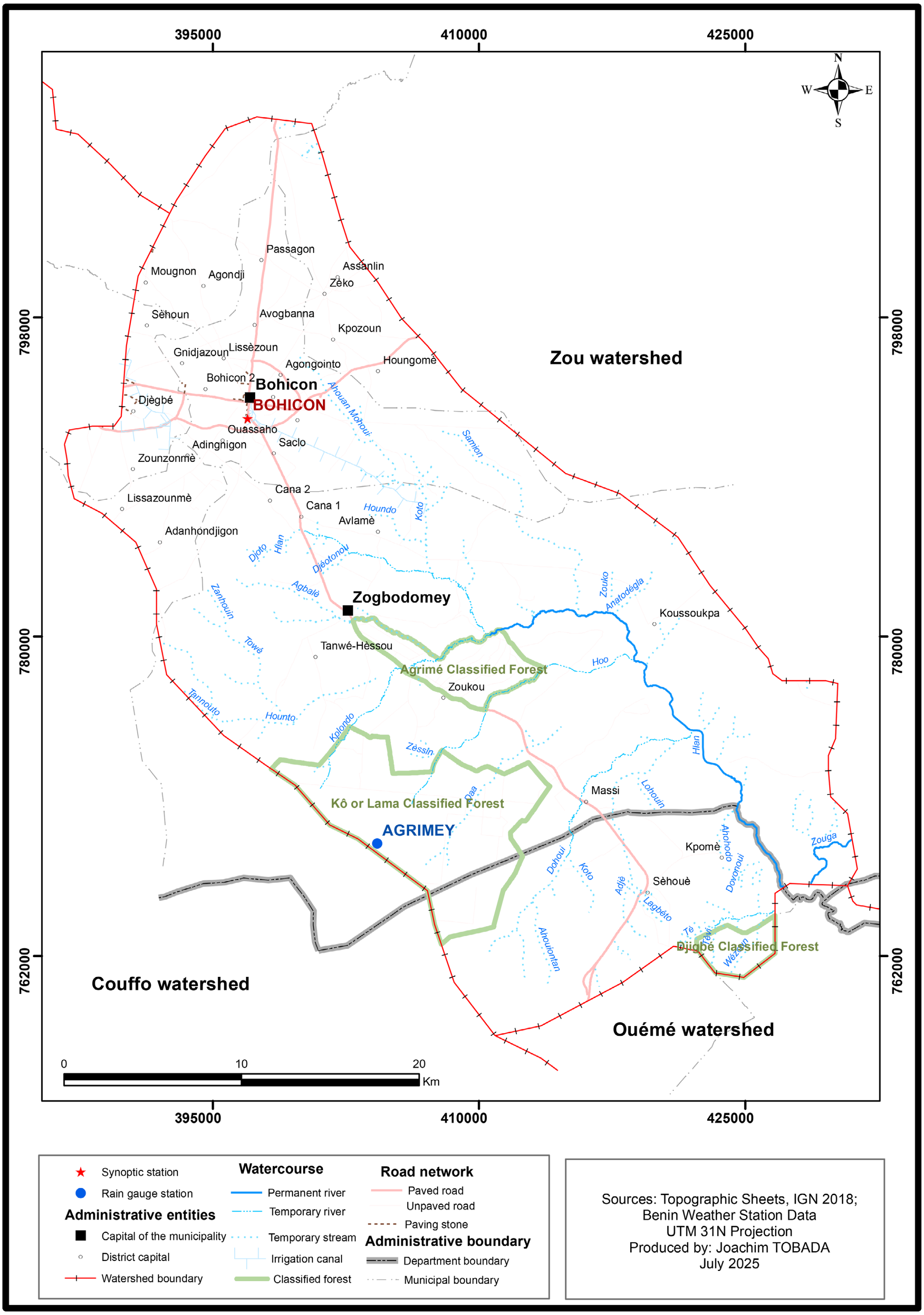


**Figure 1.** Study area map showing the Hlan watershed and surrounding hydrographic context.

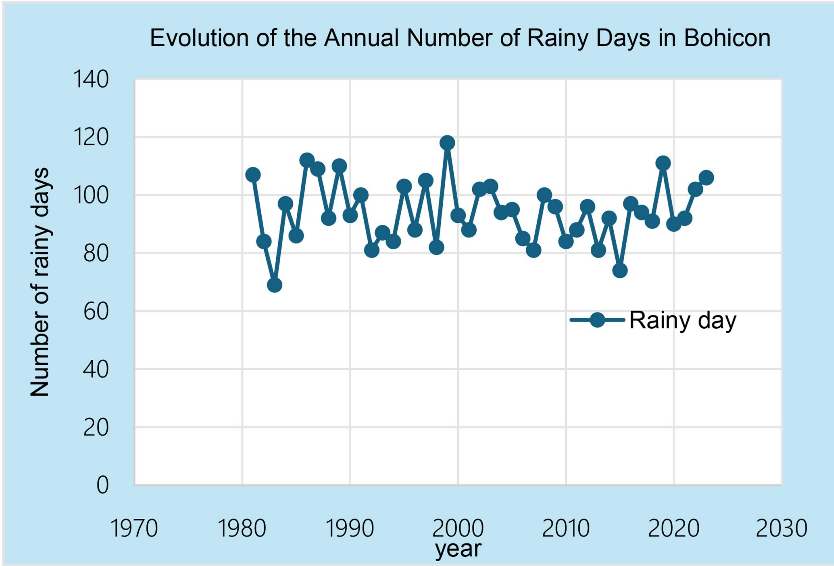


**Figure 2.** Interannual variability of the number of rainy days per year at Bohicon (1980-2023).

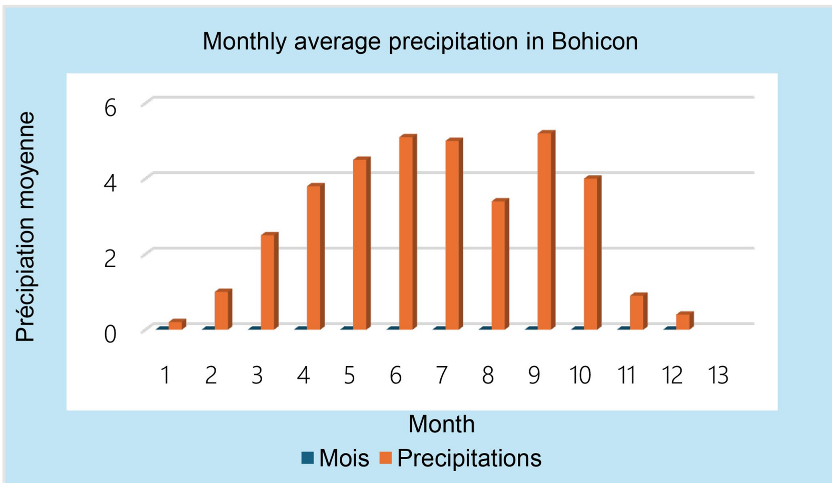


**Figure 3.** Monthly average rainfall at Bohicon, showing the bimodal rainfall regime.

Data were extracted using the NASA Giovanni portal (https://giovanni.gsfc.nasa.gov) for the spatial grid covering the Hlan watershed (latitudes 7.05˚N to 7.25˚N; longitudes 1.95˚E to 2.15˚E). To improve their local representativeness, the IMERG data were corrected for systematic bias using statistical calibration against ground-based rain gauge records.

#### 2.2.1. IMERG Data Bias Correction

To reduce systematic errors associated with satellite-based precipitation estimates, a bias correction was applied to the IMERG data prior to their use in hydrological analyses. The method adopted relies on a quantile mapping approach, which adjusts the statistical distribution of satellite-derived precipitation to match that observed on the ground, correcting both the mean bias and distributional discrepancies. The adjustment was performed on a **monthly basis** to account for seasonal variability in precipitation. Performance evaluation using statistical indicators ($R^2$, RMSE, and MAE) showed a significant improvement in the agreement between the corrected data and ground-based observations.

#### 2.2.2. Frequency Analysis Methodology

The frequency analysis began with a diagnostic assessment of the precipitation time series to verify their suitability for distribution modeling. Three standard statistical tests were applied:

- Kendall stationarity test.
- Wald-Wolfowitz runs test for independence.
- Wilcoxon homogeneity test.

These tests have been widely applied in recent hydrological studies across Africa [5].

In modeling annual maximum precipitation values, five probabilistic distributions were considered:

- Generalized Extreme Value (GEV).
- Gumbel.
- Log-normal.
- Pearson Type III.
- Weibull.

The Maximum Likelihood Estimation (MLE) method was used to estimate distribution parameters, following best practices in extreme value analysis [6].

Table 1 below presents the main probability density functions (PDFs) associated with these distributions, along with their characteristic parameters.

Table 1. Probability Density Functions (PDFs) of the tested distributions.

| Distribution | Probability Density Function (PDF) | Parameters |
|---|---|---|
| Generalized Extreme Value | $f(x)=\frac{1}{\alpha}\left[1-\frac{k}{\alpha}(x-u)\right]^{\frac{1}{k}-1}\exp\left\{-\left[1-\frac{k}{\alpha}(x-u)\right]^{\frac{1}{k}}\right\}$ | $\alpha$, $u$, $k$ |
| Gumbel | $f(x)=\frac{1}{\alpha}\exp\left[-\frac{x-u}{\alpha}-\exp\left(\frac{x-u}{\alpha}\right)\right]$ | $\alpha$, $u$ |
| Log-normal | $f(x)=\frac{1}{x\sigma\sqrt{2\pi}}\exp\left\{-\frac{(\ln x-\mu)^2}{2\sigma^2}\right\}$ | $\sigma$, $\mu$ |
| Pearson Type III | $f(x)=\frac{\alpha^{\lambda}}{\delta(\lambda)}(x-m)^{\lambda-1}e^{-\alpha(x-m)}$ | $\alpha$, $\lambda$, $m$ |
| Weibull | $f(x)=\frac{k}{\lambda}\left(\frac{x}{\lambda}\right)^{k-1}e^{-\left(\frac{x}{\lambda}\right)^{k}}$ | k, $\lambda$ |

#### 2.2.3. Model Selection Criteria

To identify the most appropriate distribution, both graphical fitting and numerical criteria were used:

- Log-likelihood (normalized).
- Akaike Information Criterion (AIC).
- Bayesian Information Criterion (BIC).

The BIC, for instance, is defined as:

$$BIC = -2\log(L) + 2k\log(N)$$

where:

- $L$ is the maximum likelihood of the model.
- $k$ is the number of parameters.
- $N$ is the sample size.

This approach follows recent recommendations for model selection under tropical hydrological conditions [7]. It was supplemented by modern Bayesian criteria such as DIC [8] and WAIC, now widely used in hydrological inference [9].

#### 2.2.4. Empirical IDF Models

The Intensity-Duration-Frequency (IDF) curves are empirical models that relate extreme rainfall intensity $i(T)$ to its duration $d$ and return period $T$. Three common models were tested:

The analytical expressions of these models are presented in **Table 2**, which summarizes their mathematical formulations and the meaning of the parameters.

**Table 2.** Empirical IDF models.

| Model Name | Formula |
|---|---|
| **Montana** | $i(T) = \frac{a(T)}{d^{\eta(T)}}$ |
| **Talbot** | $i(T) = \frac{a(T)}{\left[d + \theta(T)\right]^{\eta(T)}}$ |
| **Keifer-Chu** | $i(T) = \frac{a(T)}{d^{\eta(T)} + \theta(T)}$ |

where:

- $i(T)$ is the rainfall intensity (mm/h) for return period $T$.
- ddd is the rainfall duration (minutes).
- $a(T)$, $\eta(T)$, and $\theta(T)$ are empirical parameters.

#### 2.2.5. Model Performance Evaluation

Each IDF model was calibrated using least squares fitting, and evaluated using the following objective criteria:

The mathematical formulas of these indicators are presented in **Table 3**, in order to clarify their calculation method and their role in evaluating the performance of IDF models.

The model that exhibited the highest $R^2$, lowest RMSE, and lowest MAE was selected for generating the final site-specific IDF curves for Bohicon. This method aligns with best practices established in studies by [10] [11].

**Table 3.** Statistical performance indicators.

| Performance Indicator | Formula |
|---|---|
| Coefficient of Determination (R²) | $R^2 = 1 - \frac{\sum_{i=1}^{n}(y_i - \hat{y}_i)^2}{\sum_{i=1}^{n}(y_i - \bar{y})^2}$ |
| Root Mean Square Error (RMSE) | $\sqrt{\frac{1}{N}\sum_{i=1}^{N}(X_i - Y_i)^2}$ |
| Mean Absolute Error (MAE) | $\frac{1}{N}\sum_{i=1}^{N}\lvert X_i - Y_I \rvert$ |

## 3. Results and Discussion

### 3.1. Hypothesis Testing

To ensure the validity of the annual maximum rainfall series by duration (ranging from 30 minutes to 24 hours), three standardized statistical tests were conducted: the Kendall test for stationarity, the Wald-Wolfowitz runs test for independence, and the Wilcoxon-Mann-Whitney test for homogeneity. These tests verify the fulfillment of core assumptions required for robust frequency modeling.

- Stationarity: As shown in **Table 4**, the *p-values* obtained from the Kendall test exceed the conventional 5% significance threshold across all durations, indicating the absence of significant trends. This result confirms the stationary behavior of the time series, aligning with recommendations from [12] regarding IDF modeling in tropical climates.
- Independence: The Wald-Wolfowitz runs test values confirm that successive observations are statistically independent. All series fulfill this critical requirement, corroborating similar findings reported by [13] in studies involving GPM/IMERG satellite data.
- Homogeneity: Regarding homogeneity, the Wilcoxon-Mann-Whitney test results reveal no significant discontinuities in the means of sub-series. Except for the 2-hour and 24-hour durations, all *p-values* exceed 0.5, supporting the assumption of a globally homogeneous rainfall regime over the study period. These outcomes are consistent with the observations of [14] on bias-corrected satellite series in West Africa.

**Table 4.** Results of hypothesis testing for annual maximum rainfall intensities.

| Duration | Stationarity (Kendall) | Independence (Runs Test) | Homogeneity (Wilcoxon) |
|---|---|---|---|
| Max_30min | 0.5304 | 0.9926 | 0.902 |
| Max_1h | 0.6013 | 0.9926 | 0.8535 |
| Max_2h | 0.4639 | 0.9926 | 0.2184 |
| Max_3h | 0.9584 | 0.6757 | 0.6225 |
| Max_6h | 0.6382 | 0.6621 | 0.9509 |
| Max_24h | 0.9168 | 0.3975 | 0.3889 |

- Taken together, these results demonstrate that the datasets satisfy the three fundamental statistical assumptions—stationarity, independence, and homogeneity—required for reliable frequency analysis. This procedure aligns with current best practices outlined in recent methodological reviews on hydrological extreme value modeling [15].

Table 4 presents the results of stationarity, independence, and homogeneity tests for the maximum rainfall series at different durations.

### 3.2. Evolution of the Probability Distribution Function

Following the fitting of classical probability distributions (Gumbel, Weibull, Pearson Type III, and Lognormal) to the annual series of maximum rainfall intensities for each duration, the quality of the fit was assessed using two complementary statistical criteria:

- Kolmogorov-Smirnov Test (p_KS): This evaluates the maximum deviation between the empirical and the fitted theoretical distributions. A *p-value* greater than 0.05 indicates that the null hypothesis (good conformity) is not rejected, implying an acceptable statistical fit.
- Akaike Information Criterion (AIC): This criterion allows for an objective comparison of models by balancing goodness-of-fit with model complexity.

Table 5 below presents the values obtained for the p_KS and AIC criteria according to different recording durations. It allows identifying the probability distributions that best fit the annual maximum intensity series.

**Table 5.** Statistical metrics for goodness-of-fit evaluation.

| Duration | Best-fitting distribution | p_KS | AIC |
|---|---|---|---|
| Max_30min | Weibull | 0.8822 | 134.58 |
| Max_1h | Gumbel | 0.5546 | 143.05 |
| Max_2h | Gumbel | 0.9928 | 180.44 |
| Max_3h | Gumbel | 0.8948 | 188.77 |
| Max_6h | Gumbel | 0.2182 | 191.1 |
| Max_24h | Gumbel | 0.699 | 213.84 |

These results confirm the necessity of duration-specific model selection, based on robust statistical indicators. They align with findings from [16] [17], who emphasized the variability in the best-fitting distributions depending on the temporal scale considered.

Visual Validation with Q-Q Plots

To complement the numerical analysis, visual validation of the selected models was carried out using quantile-quantile (Q-Q) plots. These graphs compare the empirical quantiles of observed data with the theoretical quantiles of the fitted distributions. A strong alignment along the identity line (red dashed line) indicates a good fit.

As illustrated in **Figure 4**, the Q-Q plots generally confirm the suitability of the selected probability distributions, particularly the Weibull and Gumbel laws. These distributions successfully replicate the variability observed in maximum rainfall intensities across all durations.

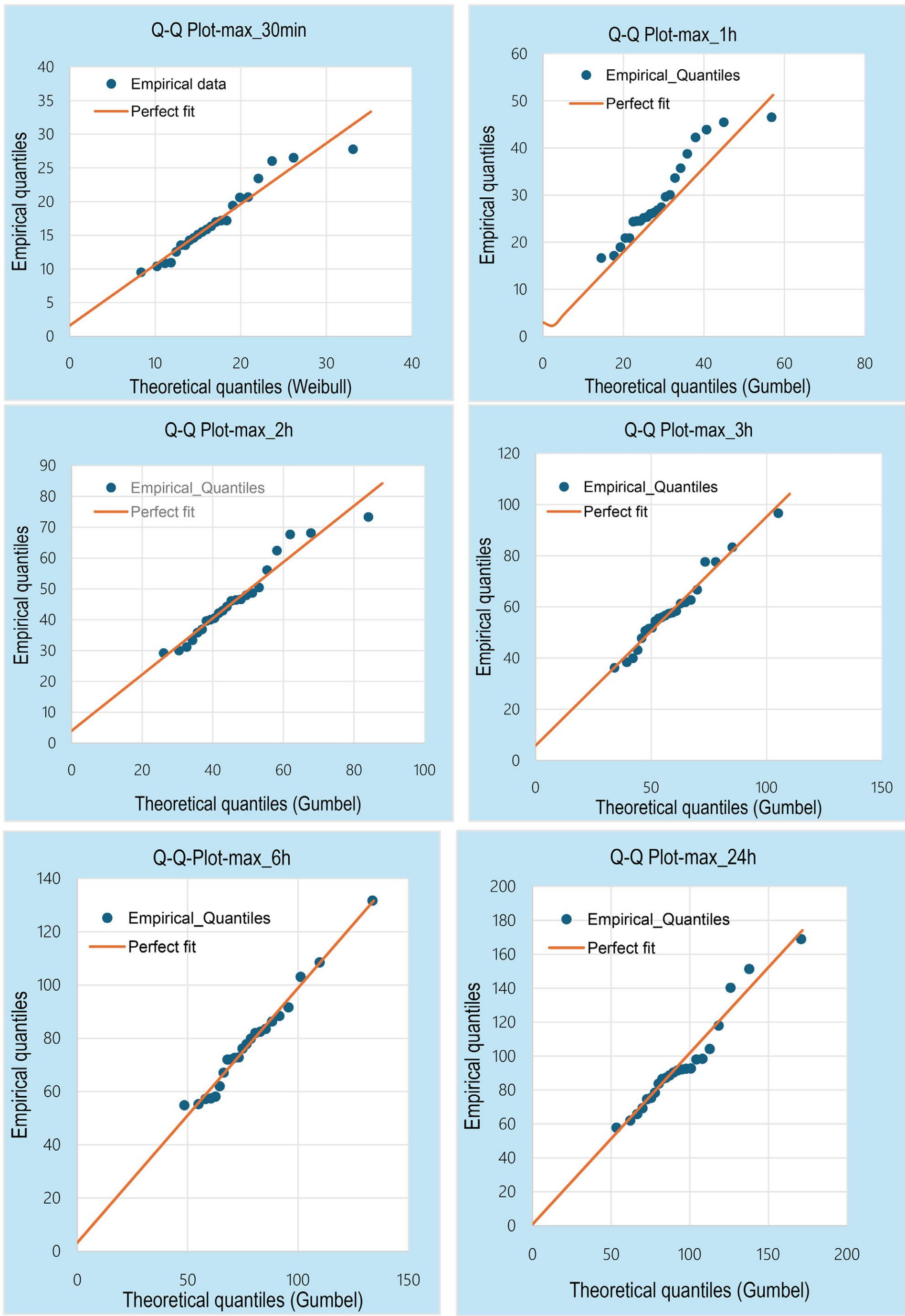


**Note:** Subplots include Q-Q plots for durations of 30 minutes, 1 hour, 2 hours, 3 hours, 6 hours, and 24 hours. The empirical quantiles (blue dots) are plotted against the theoretical quantiles derived from the selected probability distributions.

**Figure 4.** Q-Q plots of empirical vs. theoretical quantiles for all durations.

### 3.3. Comparative Assessment of the Montana, Talbot, and Keifer-Chu Models

The performance evaluation of three empirical Intensity-Duration-Frequency (IDF) models—Montana, Talbot, **and** Keifer-Chu—was conducted using the statistical indicators coefficient of determination ($R^2$), Root Mean Square Error (RMSE), and Mean Absolute Error (MAE). This methodology follows the recommendations, which emphasize multi-criteria performance evaluation of IDF formulations under varying return periods.

#### 3.3.1. Talbot Model Performance

As shown in Table 6, the Talbot model consistently delivers the best fit across all return periods. For a 2-year return period, it achieves a very high $R^2$ value of 0.962, with relatively low error levels (RMSE = 4.90, MAE = 4.10). Even in the 100-year return period, its performance remains satisfactory ($R^2 = 0.813$), with significantly lower errors than those obtained from the Montana and Keifer-Chu models.

These results validate the robustness of the Talbot formulation in capturing both short- and long-duration rainfall extremes in the Bohicon region, consistent with findings by [18] on the importance of model resilience under extreme events.

Table 6 presents the performance metrics ($R^2$, RMSE, and MAE) of the IDF Talbot model for different return periods (T).

**Table 6.** Talbot model evaluation metrics.

| Return Period (T) | $R^2$ | RMSE | MAE |
|---|---|---|---|
| 2 years | 0.962 | 4.90 | 4.10 |
| 5 years | 0.942 | 7.95 | 6.30 |
| 10 years | 0.912 | 11.02 | 8.20 |
| 20 years | 0.884 | 14.55 | 10.85 |
| 50 years | 0.843 | 19.75 | 14.80 |
| 100 years | 0.813 | 23.90 | 17.85 |

**Table 7.** Keifer-Chu model evaluation metrics.

| Return Period (T) | $R^2$ | RMSE | MAE |
|---|---|---|---|
| 2 years | 0.954 | 5.45 | 4.50 |
| 5 years | 0.928 | 8.45 | 6.90 |
| 10 years | 0.895 | 11.80 | 9.10 |
| 20 years | 0.860 | 15.65 | 11.75 |
| 50 years | 0.812 | 21.20 | 15.90 |
| 100 years | 0.779 | 26.05 | 19.20 |

#### 3.3.2. Keifer-Chu Model Performance

The Keifer-Chu model, while mathematically close to Talbot's formulation, demonstrates slightly reduced predictive performance, particularly for high return periods. As shown in Table 7, the $R^2$ drops to 0.779 for T = 100 years, accompanied by larger RMSE and MAE values. This behavior aligns with observations by [18], who highlighted the sensitivity of empirical models to extremes and the limitations in extrapolation accuracy.

Table 7 presents the evaluation metrics ($R^2$, RMSE, and MAE) of the Keifer-Chu model for different return periods (T).

#### 3.3.3. Montana Model Performance

The Montana model, though simpler and historically widespread due to its two-parameter structure, proves to be the least effective among the three models assessed. It shows significant limitations in representing high-intensity events and long durations. As detailed in Table 8, $R^2$ drops to 0.725 for a 100-year return period, and the associated error metrics (RMSE and MAE) are substantially higher than those of the Talbot and Keifer-Chu models. These limitations corroborate the findings of [19], who questioned the adequacy of low-parameter models in capturing tail behaviors of extreme hydrological distributions.

Table 8 presents the evaluation metrics ($R^2$, RMSE, and MAE) of the Montana model for different return periods (T).

**Table 8.** Montana model evaluation metrics.

| Return Period (T) | $R^2$ | RMSE | MAE |
|---|---|---|---|
| 2 years | 0.898 | 8.08 | 7.54 |
| 5 years | 0.872 | 11.47 | 9.98 |
| 10 years | 0.840 | 14.83 | 12.29 |
| 20 years | 0.804 | 18.72 | 15.01 |
| 50 years | 0.758 | 24.40 | 18.81 |
| 100 years | 0.725 | 29.00 | 21.81 |

These comparative results clearly support the Talbot model as the most appropriate choice for IDF curve construction in Bohicon's context. Its superior fitting capacity across return periods, along with its low error metrics, make it a robust and reliable option for the design of urban drainage infrastructure under climate uncertainty.

### 3.4. Analysis of Simulated Rainfall Intensities According to Duration and Return Periods

The Intensity-Duration-Frequency (IDF) matrix (see Table 9) reveals a consistent pattern where rainfall intensity decreases as the duration increases, while intensity logically increases with the return period. This inverse relationship between intensity and duration, and the direct relationship with return period, is a characteristic behavior of tropical rainfall regimes, in which short-duration events tend to be more intense and violent [20].

In particular, the difference in intensity between short (e.g., 0.5 h and 1 h) and long return periods (e.g., 100 years) is most pronounced for shorter durations.

This confirms that extreme events disproportionately affect short and highly concentrated rainfall episodes, a phenomenon that is critical in understanding flash flooding risks in tropical urban environments.

These findings are consistent with the conclusions, who emphasized the pivotal role of short-duration rainfall in urban flood modeling. Moreover, the influence of the return period tends to diminish as the duration increases, a trend widely recognized in recent hydrological literature [21]. Such behavior underscores the need for regionally calibrated IDF curves that reflect the spatio-temporal variability of extreme precipitation events.

The corresponding simulated intensity values for each duration and return period are presented in **Table 9**, which illustrates the quantitative distribution of precipitation intensities derived from the fitted IDF model.

**Table 9.** Rainfall intensity quantiles (mm/h) for various return periods and durations.

| Duration (hours) | 2 years | 5 years | 10 years | 20 years | 50 years | 100 years |
|---|---|---|---|---|---|---|
| 0.5 | 32.012 | 41.177 | 47.246 | 53.066 | 60.601 | 66.247 |
| 1.0 | 27.606 | 35.431 | 40.613 | 45.583 | 52.016 | 56.837 |
| 2.0 | 21.999 | 27.364 | 30.916 | 34.323 | 38.734 | 42.038 |
| 3.0 | 18.691 | 23.062 | 25.957 | 28.733 | 32.326 | 35.019 |
| 6.0 | 12.471 | 15.097 | 16.835 | 18.503 | 20.662 | 22.280 |
| 24.0 | 3.734 | 4.639 | 5.238 | 5.813 | 6.557 | 7.114 |

The structure observed in **Table 9** aligns well with tropical hydrological dynamics and confirms the critical importance of accurate IDF curve calibration per region. Given the sensitivity of urban hydrological systems to rainfall intensity and concentration, especially for stormwater infrastructure design, these findings provide essential guidance for planners and engineers operating in similar climatic zones.

### 3.5. Hydrological Analysis of Calibrated Talbot Model Parameters

The analysis of the adjusted parameters of the Talbot model reveals consistent trends from a hydrological perspective. As shown in **Table 10**, the parameter $a$, which reflects the maximum rainfall intensity, increases progressively with the return period (T). This upward trend indicates the intensification of extreme precipitation events over time, highlighting the increasing magnitude of rare storms.

Conversely, the exponent parameter $\eta$ exhibits a slight decrease as the return period increases, suggesting that intensity decreases more slowly with duration for rare events. This behavior implies that longer storm events remain relatively intense during extreme return periods.

In parallel, the offset parameter $\theta$ shows a decreasing pattern, indicating a greater concentration of rainfall over shorter durations as the rarity of the event increases. This tendency underscores the abrupt and focused nature of extreme precipitation in tropical regions; a phenomenon frequently associated with flash flooding risks.

These parameter evolutions confirm the Talbot model's ability to capture the non-linear dynamics of extreme rainfall patterns in the studied region. They are consistent with hydrological expectations for tropical climates and validate the model's applicability in the local IDF (Intensity-Duration-Frequency) framework.

The corresponding values of these parameters are presented in **Table 10**, which summarizes the estimated Talbot coefficients for the different return periods and the corresponding IDF curves.

**Table 10.** Calibrated talbot model coefficients by return period.

| Return Period (years) | 2 | 5 | 10 | 20 | 50 | 100 |
|---|---|---|---|---|---|---|
| $a$ | 123.11 | 127.32 | 135.36 | 144.72 | 158.17 | 168.86 |
| $\eta$ | 1.04 | 1.00 | 0.98 | 0.98 | 0.97 | 0.97 |
| $\theta$ | 3.17 | 2.61 | 2.42 | 2.29 | 2.18 | 2.12 |

### 3.6. Hydrological Analysis of Simulated IDF Curves and Comparison with Regional References

The IDF curve presented illustrates the evolution of rainfall intensities as a function of duration for different return periods (from 2 to 100 years). It highlights a classic but significant trend: the longer the rainfall duration, the lower the intensity, and the longer the return period, the higher the intensity. This dual temporal decrease and frequency increase accurately reflects the expected behavior of extreme events in a tropical urban context, such as that of Bohicon. The maximum intensity for a duration of 30 minutes varies from approximately 32 mm/h for T = 2 years to more than 66 mm/h for T = 100 years, representing an increase of over 100%, which demonstrates a high potential for urban runoff during rare events. This rapid increase in intensity over short periods and with high recurrence corroborates the recent, which highlight the increased vulnerability of African cities under the combined effect of climate change and rapid urbanization.

The use of a 30-minute temporal resolution for constructing IDF curves represents a significant methodological advancement compared to traditional approaches based on hourly or daily time steps. This temporal precision allows for a better capture of short-duration rainfall intensities, often responsible for flash floods in urban areas. In the context of the cities of Abomey and Bohicon, where drainage networks have limited capacity and very short times of concentration, taking into account high-frequency rainfall is essential to accurately reproduce runoff dynamics. Rainfall events lasting less than an hour generate rapid peak flows, which can overwhelm infrastructure and amplify flood risks. This approach thus strengthens the reliability of hydrodynamic simulations and the relevance of planning strategies aimed at reducing vulnerability to intense urban flooding.

The simulated rainfall intensities in Bohicon are compared to previous studies conducted in Cotonou [22] [23], a comparison justified by the geographical proximity and similarity of the climatic regimes of the two southern Benin locations.

Situated in the humid subequatorial zone, these cities exhibit a bimodal regime and often experience intense, convective rainfall. This regional perspective allows us to assess the spatial consistency of the IDF parameters, to understand the discrepancies related to topography or local rainfall dynamics, and to strengthen the validity of the results obtained in Bohicon, while also shedding light on the regional variability of extreme rainfall.

Compared to the empirical models used, the three-parameter Talbot model proves more robust than the two-parameter Montana model, particularly for short-duration, high-intensity events. This superiority is explained by the third parameter, which allows for better control of the hyetograph shape and rainfall concentration. In the context of Bohicon's highly variable, convective tropical rainfall, this parameter gives the Talbot model greater flexibility in reproducing the rapid decrease in intensity over time and the increase with the return period. This results in higher $R^2$ values and lower errors (RMSE and MAE) compared to the Montana model. The addition of this parameter is not merely a statistical improvement; it provides a better physical representation of extreme events, essential for the realistic design of urban drainage structures.

Overall, the study shows that the IDF curves constructed at high temporal resolution (30 minutes), calibrated with the Talbot model, offer a reliable and robust representation of extreme rainfall in Bohicon. The regional comparison with Cotonou and the analysis of model performance confirm the scientific and operational relevance of this approach for the design of critical infrastructure and the management of urban flooding in southern Benin.

The curves shown in **Figure 5** illustrate the relationship between intensity and duration for different return periods. They reveal an almost exponential decrease in intensities as duration increases, reflecting a marked concentration of extreme rainfall in short-duration events.

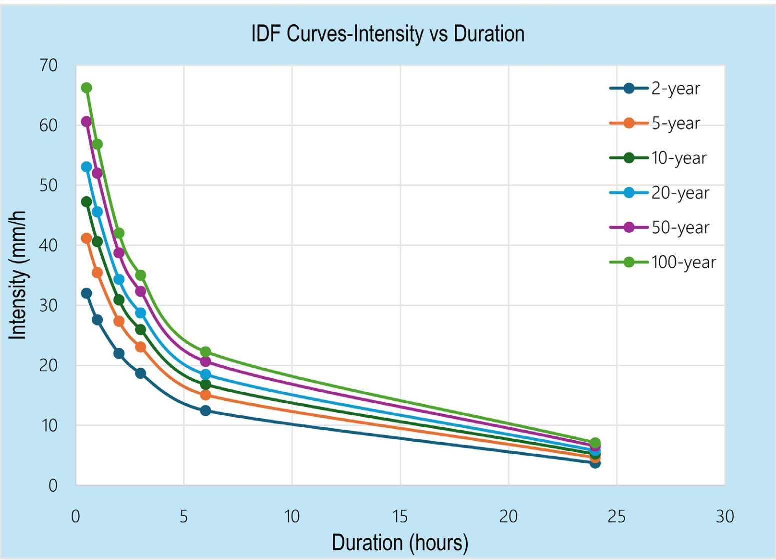


**Figure 5.** IDF curve—rainfall intensity vs duration.

Figure 6, plotted on a logarithmic scale, provides a clearer visualization of this trend and highlights the consistency of the Talbot model fits across all considered durations.

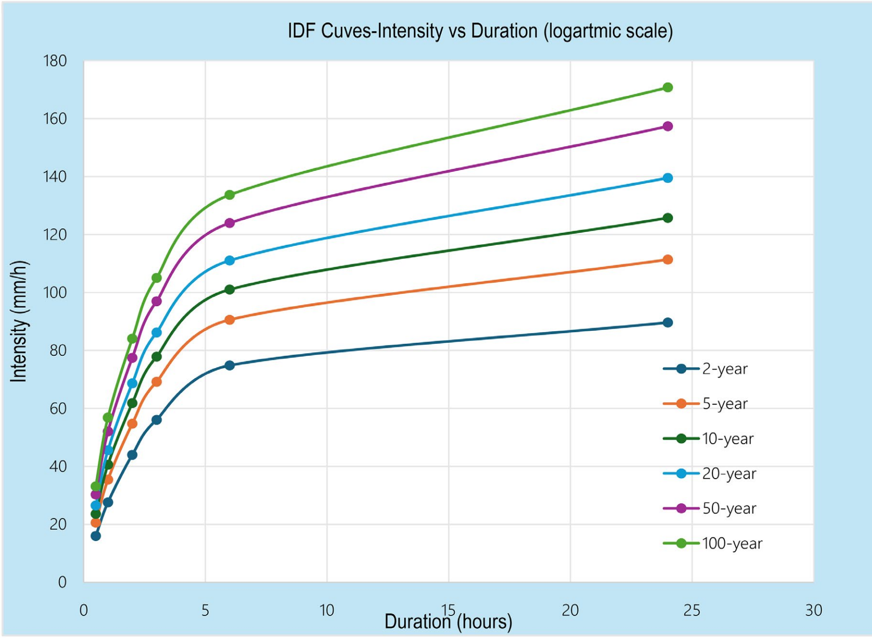


Figure 6. Log-scale IDF curves—intensity vs duration.

## 6. Conclusions

This study enabled the development of updated Intensity-Duration-Frequency (IDF) curves for the synoptic station of Bohicon (Benin), based on corrected IMERG satellite data covering a recent period. The analysis of these data, combined with rigorous fitting to probability distributions, particularly the Gumbel distribution, allowed for the generation of representative IDF curves suitable for hydraulic modeling of urban flooding.

The empirical Montana, Keifer-Chu, and Talbot models were tested, and the three-parameter Talbot model proved to be the most effective, with low statistical errors and coefficients of determination greater than 0.95. These curves accurately reflect the dynamics of extreme rainfall in the Sudanese-Guinean urban context of Bohicon. The third parameter of the Talbot model allows for a better representation of rainfall concentration and the rapid decrease in intensity over time, thus giving the model greater flexibility to capture rare, high-intensity events.

Comparison with older IDF curves, particularly those established by the CIEH before 1984, reveals significant differences. For example, for a one-hour rainfall event with a 10-year return period, the estimated intensity increases from 62 mm/h according to the older curves to 84 mm/h with the newer curves, representing an increase of nearly 35%, illustrating the high potential for urban runoff associated with extreme events. These older curves, based on limited time series, do not take into account recent changes in rainfall patterns, exposing urban areas to an increased risk of flooding if they continue to be used for designing infrastructure.

The new IDF curves thus provide an updated and reliable basis for feeding urban hydraulic models such as HEC-RAS, SWMM, or HEC-HMS, enabling the simulation of surface runoff, the assessment of flood zones, and the resizing of drainage structures according to extreme hazards. They contribute to adapting development projects to contemporary climate realities, within a framework of urban resilience and sustainable flood risk management.

## Conflicts of Interest

The authors declare no conflicts of interest regarding the publication of this paper.

## References

[1] Comité Interafricain d'Études Hydrauliques (CIEH) (1984) Étude des courbes de fréquence des précipitations en Afrique de l'Ouest et du Centre.

[2] World Meteorological Organization (WMO) (2021) WMO Assessment Guidelines for Improving NHS capabilities in Flood Forecasting and Warning. https://www.floodmanagement.info/floodmanagement/wp-content/uploads/2021/01/WMO-Brochure_final_June-2021.pdf

[3] Hounkpè, J. (2023) Assessment of Extreme Rainfall Events and Their Hydrological Impacts in West Africa. *Journal of Hydrology*: *Regional Studies*, **45**, 101-120.

[4] Diedhiou, A. (2018) Climate Change and Climate Variability in West Africa. *WIREs Climate Change*, **9**, 497.

[5] Lebartier (2004) Choix de modèles en statistique: Critères d'information et inférence bayésienne. INRA.

[6] Koutsoyiannis, D. (2020) Extreme Value Analysis in Hydrology: Revisited and Extended. *Water Resources Research*, **24**, 3899-3932.

[7] Watanabe, S. (2012) Asymptotic Equivalence of Bayes Cross Validation and Widely Applicable Information Criterion in Singular Learning Theory. *Journal of Machine Learning Research*, **11**, 3571-3595.

[8] Spiegelhalter, D.J., Best, N.G., Carlin, B.P. and Van Der Linde, A. (2002) Bayesian Measures of Model Complexity and Fit. *Journal of the Royal Statistical Society Series B*: *Statistical Methodology*, **64**, 583-639. https://doi.org/10.1111/1467-9868.00353

[9] Vehtari, A., Gelman, A. and Gabry, J. (2017) Practical Bayesian Model Evaluation Using Leave-One-Out Cross-Validation and WAIC. *Statistics and Computing*, **27**, 1413-1432. https://doi.org/10.1007/s11222-016-9696-4

[10] Shamshirband, F.A. (2020) Extreme Rainfall Forecasting Using Machine Learning Models. *Atmospheric Research*, **245**, Article 105122.

[11] Zhang, D. (2022) Spatiotemporal Variation of Extreme Precipitation under Climate Change. *International Journal of Climatology*, **42**, 2567-2583.

[12] Abdolalizadeh, B. (2021) Assessment and Monitoring of Natural Atmospheric Hazards (Heavy Rainfall) in the Cities of Northwestern Iran Using Satellite Data. *Carpathian Journal of Earth and Environmental Sciences*, **16**, 423-436.

[13] Silva, T. (2022) Evaluating Homogeneity and Trends in Extreme Daily Precipitation Indices in a Semiarid Region of Brazil. *Frontiers in Earth Science*, **10**, 1-20.

[14] Getachew Feleke, A. and Abera, M. (2020) Analysis of Rainfall and Temperature

Trends and Variability in Semi-Arid North-Eastern Ethiopia. *International Journal of Environmental Monitoring and Analysis*, **8**, 75-87.
https://doi.org/10.11648/j.ijema.20200804.11

[15] Zhang, X., Wang, G., *et al*. (2021) Example: Advances in Satellite Rainfall Estimation. *Journal of Hydrology*, **600**, Article 127150.

[16] Goula, T.A., Soro, G.E., Dao, A., *et al*. (2010) Frequency Analysis and New Cartography of Extremes Daily Rainfall Events in Côte d'Ivoire. *Journal of Applied Sciences*, **2**, 6004-6015.

[17] An, D., Eggeling, J., Zhang, L., He, H., Sapkota, A., Wang, Y., *et al*. (2023) Extreme Precipitation Patterns in the Asia-Pacific Region and Its Correlation with El Niño-Southern Oscillation (ENSO). *Scientific Reports*, **13**, Article No. 11068.
https://doi.org/10.1038/s41598-023-38317-0

[18] Naveau, A. (2016) A Non-Parametric Rainfall Frequency Analysis Using Extreme Value Theory. *Water Resources Research*, **52**, 2753-2769.

[19] Koutsoyiannis, D. (2015) Negligent Use of Climate Change Projections in Hydrologic Design. *Water Resources Research*, **51**, 2937-2948.

[20] Schwarz, G. (1978) Estimating the Dimension of a Model. *The Annals of Statistics*, **6**, 461-464.
https://doi.org/10.1214/aos/1176344136

[21] Singh, V.P. (2009) Derivation of Intensity Duration Frequency Relationship using Scaling Theory. *Water Resources Management*, **23**, 461-464.

[22] Paturel, J.E. (1997) The Influence of Climate Variability on Regional Hydrology. IAHS Publication.

[23] Djaman, C. (2019) Rainfall Intensity-Duration-Frequency Relationships in Cotonou. *Hydrological Sciences Journal*, **64**, 837-849.